

# FREQUENCY-DEPENDENT BRANCHING RATIO IN THE INFRARED MULTIPHOTON PHOTOCHEMISTRY OF DIETHYL CARBONATES

WILLIAM E. FARNETH

*E. I. du Pont de Nemours and Company, Central Research and Development Department, Experimental Station 356|231, Wilmington, Delaware 19898, USA*

MARCUS W. THOMSEN\* AND THOMAS L. BECK

*Chemistry Department, Franklin and Marshall College, Lancaster, Pennsylvania 17604, USA*

Unimolecular decomposition of 0.1 Torr of diethyl carbonate, diethyl- $d_5$  carbonate and diethyl- $d_{10}$  carbonate induced by irradiation with a CO<sub>2</sub> TEA laser was investigated. In all cases only ethylene, ethanol and CO<sub>2</sub> were obtained. In the case of diethyl- $d_5$  carbonate, both ethylene- $d_4$  and ethylene- $d_0$  were observed together with the corresponding isotopic variants of ethanol. The chemical branching ratio was determined as a function of irradiation frequency and laser fluence by analysis of the ethylene- $d_0$ /ethylene- $d_4$  ratio. RRKM theory applied to the branching ratio data requires very different average energies for two sets of fluence and frequency conditions that give identical total yields.

## INTRODUCTION

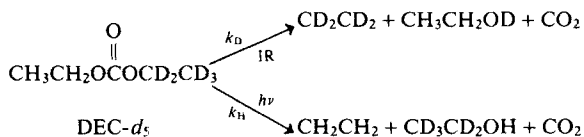
Investigations of the infrared photochemistry of molecules that can decompose by more than one reaction pathway have proved to be especially useful in characterizing the multiphoton activation process.<sup>1-10</sup> Branching ratios from multichannel reactions are a sensitive function of the energy content of the reacting molecules. Comparison of the observed branching ratio with the predictions of statistical unimolecular rate theories allows the average energy of reacting molecules,  $\langle E_r \rangle$ , to be determined.<sup>1,2</sup> The change in branching ratio resulting from systematic variation in experimental parameters (e.g. laser fluence, laser intensity or bath gas pressure) constitutes perhaps the best available data on how sensitive  $\langle E_r \rangle$  is to these parameters. This important information is useful for developing predictive versions of rate equation models of infrared multiphoton photochemistry,<sup>11-13</sup> and for designing infrared photochemistry experiments that yield one reaction pathway preferentially.<sup>14</sup>

One variable that has not been very thoroughly examined with respect to its effect on  $\langle E_r \rangle$  is laser frequency. Theoretical models of multiphoton decom-

position suggest that the average energy of reacting molecules should depend on the rates of absorption, chemical reaction and deactivation.<sup>11</sup> Laser frequency influences  $\langle E_r \rangle$  through its effect on the rate of photon absorption. The rate of absorption from level  $i$  to level  $j$  is given by  $R_{ij} = I\sigma_{ij}N_i$  where  $N_i$  is the population of molecules in the absorbing level,  $I$  is the laser intensity, and  $\sigma_{ij}$  is the absorption cross-section for the particular  $j \leftarrow i$  transition. In the energy regime above the reaction threshold photons will continue to be absorbed until  $R_{ij} \approx k(E_i)N_i$ , the unimolecular reaction rate at energy  $E_i$ . When the branching ratio changes in response to changes in experimental parameters, information on how those parameters influence the up-pumping rates,  $R_{ij}$ , can be inferred.

In this paper we describe the infrared photochemistry of both diethyl-1,1,1,2,2- $d_5$  carbonate (DEC- $d_5$ ), a molecule with two unimolecular reaction channels that differ only by isotopic substitution, and the parent molecule DEC- $d_0$ . The experiment is conceptually similar to work reported by other groups.<sup>2,9,10</sup> DEC- $d_5$  is an especially attractive molecule for this type of study for several reasons. (1) The two competitive reaction channels ( $k_H$  and  $k_D$ , Scheme 1) both yield stable, molecular products via mechanisms that are well established.<sup>15</sup>

\* Author for correspondence.



(2) The thermal chemistry of both DEC- $d_0$ <sup>16</sup> and DEC- $d_5$  are well characterized and the Arrhenius parameters for both channels from DEC- $d_5$  have been determined.<sup>17</sup> This permits accurate RRKM calculations of the branching ratio as a function of internal energy to be performed. (3) DEC- $d_5$  possesses two distinct absorption bands in the region accessible with the CO<sub>2</sub> laser. (4) The molecule is closely related in structure to ethyl acetate, which is one of the most thoroughly investigated single-channel organic reactants in multiphoton photochemistry.<sup>18,19</sup> As a class, organic esters are important infrared photochemical reagents because of strong absorptions in the CO<sub>2</sub> laser region and useful unimolecular chemistry; pyrolysis of esters is a classical preparative method for olefins.<sup>20</sup>

### EXPERIMENTAL

DEC- $d_5$  was prepared via the reaction of ethanol- $d_6$  (Stohler Isotope Chemicals, 99% D) with ethyl chloroformate (MCB Chemicals). Reaction was performed at 4–6 °C in methylene chloride solution containing pyridine (1 equiv.). The product was purified by preparative gas chromatography (GC). Mass spectral (MS) analysis (Finnegan 4000-EI) gave  $m/z = 96, 45, 93, 46, 50, 123, 124$  in order of decreasing intensity. No peak is observed at  $m/z 118–122$  ( $M^+$  of DEC- $d_0$ ). IR (gas, Beckmann IR 4250): 2800–3050, 2100–2300, 1760, 1375, 1295, 1200, 1095, 1060, 1025, 990, 880  $\text{cm}^{-1}$ .

DEC- $d_{10}$  was prepared by refluxing 2.2 equiv. of ethanol- $d_6$  with carbonylimidazole (Aldrich) for 1 h followed by distillation).

Infrared photochemical experiments were performed on vapor-phase samples of the diethyl carbonates in a cylindrical Pyrex vessel (7.5 cm × 2.5 cm i.d.) fitted with KCl or NaCl windows. Sample pressures were measured with an MKS-Baratron 220 capacitance manometer. The samples were irradiated with a collimated beam from a Lumonics CO<sub>2</sub> TEA-101 laser, which was operated multimode. The beam emerging from the laser was reduced to 25 mm diameter with an iris and telescoped to 7 mm diameter with a combination of two ZnSe lenses. The beam was characterized using a Laser Precision KT-1510 pyroelectric detector, a Scientech (Model 38-0102) volume-absorbing calorimeter and an Optical Engineering 16A spectrum analyzer. At both experimental frequencies the pulse consisted of an initial *ca* 200-ns spike with a tail to *ca* 1.5  $\mu\text{s}$ . The spatial characteristics of the beam were

determined by two methods: (i) the beam was subdivided into quadrants, the fraction of laser energy in each quadrant being independent of frequency, and (ii) the intensity cross-section was obtained by moving a pinhole aperture across the horizontal and vertical axes of the beam. The profiles obtained by the latter method were roughly trapezoidal for both axes and identical within experimental error at the two experimental frequencies. When necessary, the laser beam was attenuated with a gas cell containing variable pressures of an absorbing material.

Reaction yields and product ratios were determined by GC [Varian 2400 equipped with an HP-3390A integrator, using 10% Carbowax 1540 on Chromosorb (60–80 mesh), 10 ft × 1/8 in i.d. column) GC–MS (Hitachi RMU-6MS) or GC–Fourier transform infrared spectroscopy (Digilabs FTS-10). The branching ratio was most conveniently determined from FTIR spectra of the photolysis mixture. Absorption intensities were determined at 950 and 722  $\text{cm}^{-1}$ , the Q-branch maxima of the CH<sub>2</sub> and CD<sub>2</sub> out-of-plane deformation modes of ethylene- $d_0$  and ethylene- $d_4$ , respectively. Spectral subtraction of DEC- $d_5$  and/or ethanol- $d_0$  or - $d_6$  did not change the absorbance ratios appreciably. The ratio of absorbances was converted to a concentration ratio using the Beer–Lambert Law. Absorptivities of C<sub>2</sub>H<sub>4</sub> and C<sub>2</sub>D<sub>4</sub> at these frequencies were obtained from C<sub>2</sub>H<sub>4</sub>–C<sub>2</sub>D<sub>4</sub> mixtures at similar pressures and under analytical conditions identical with those used in photochemical product analyses. Comparable results for branching ratios could be obtained by analyzing ethanol- $d_0$  and - $d_5$  at specific frequencies between 3000–2900 and 2250–2100  $\text{cm}^{-1}$  using GC–FTIR.

### RESULTS AND DISCUSSION

The infrared photochemistry of three isotopomers of DEC, DEC- $d_0$ , DEC- $d_5$  and DEC- $d_{10}$ , was examined. In DEC- $d_5$  one of the two ethyl groups is completely deuterated. In DEC- $d_{10}$  all hydrogens are replaced by deuterium. The infrared spectra of DEC- $d_0$ , DEC- $d_5$  and DEC- $d_{10}$  are given in Figure 1. Significant differences are evident in these spectra in the region accessible with a CO<sub>2</sub> TEA laser (900–1100  $\text{cm}^{-1}$ ). The band centered at 1378  $\text{cm}^{-1}$  (CH<sub>3</sub> deformation) in DEC- $d_0$  splits into two bands at 1377 and 1056  $\text{cm}^{-1}$  in DEC- $d_5$  and disappears completely in favor of the lower frequency band in DEC- $d_{10}$ . Bands appearing at 1056 ± 9  $\text{cm}^{-1}$  for compounds structurally similar to DEC- $d_5$  have been assigned as CD<sub>3</sub> deformations.<sup>21–23</sup> Similarly, the band at 1031  $\text{cm}^{-1}$  in DEC- $d_0$  appears to split into two bands at 1029 and 994  $\text{cm}^{-1}$  in DEC- $d_5$ . In DEC- $d_{10}$  a single band at 1016  $\text{cm}^{-1}$  appears in this region. The 1031  $\text{cm}^{-1}$  band in DEC- $d_0$  has been assigned as an O–C(H<sub>2</sub>) stretch.<sup>24</sup> Changes observed in the DEC- $d_5$  spectrum appear to be consistent with this

assignment (reduced mass ratios indicate that an O-CH<sub>2</sub> stretch at 1031 cm<sup>-1</sup> should shift to 996 cm<sup>-1</sup> on deuterium substitution).

The infrared photodecomposition of the diethyl carbonates leads cleanly to the three products expected from pyrolysis studies, ethanol, ethylene and CO<sub>2</sub>.<sup>16</sup> When DEC-*d*<sub>5</sub> is the reactant, branching occurs to yield both ethylene-*d*<sub>0</sub> and ethylene-*d*<sub>4</sub> together with the corresponding isotopic ethanols and CO<sub>2</sub> (Scheme 1). For each isotopomer and under all experimental conditions

the ethanol-to-ethylene ratio was 1.02 ± 0.08. Irradiation of ethanol or ethanol-*d*<sub>6</sub> under identical photolysis conditions gave insignificant decomposition. Therefore, ethanol and ethylene are produced in equivalent amounts from DEC, and there is no significant secondary photochemistry. Scheme 1 adequately represents all routes to ethylene.

Photochemical reaction was investigated at two frequencies with each isotopomer: *P*(14), 1052 cm<sup>-1</sup>, and *P*(38), 1029 cm<sup>-1</sup>. Irradiation was generally done with

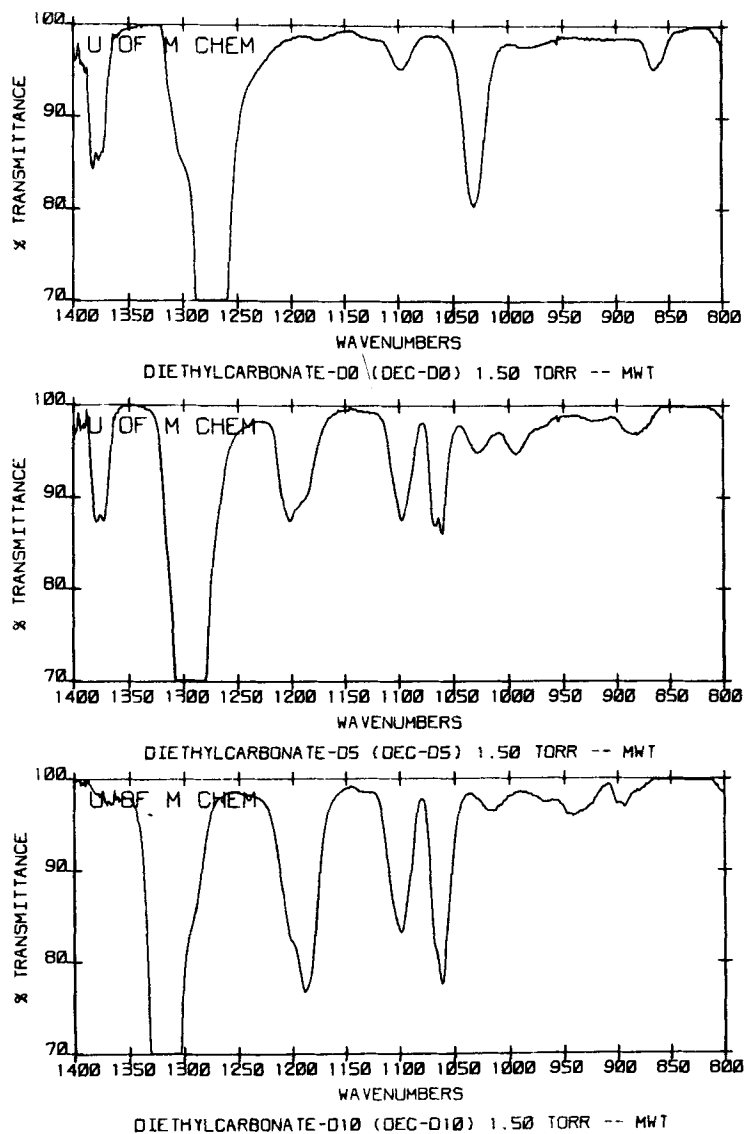


Figure 1. Vapor-phase infrared spectra of DEC-*d*<sub>0</sub>, DEC-*d*<sub>5</sub> and DEC-*d*<sub>10</sub>. The irradiation frequencies, *P*(38), 1052 cm<sup>-1</sup>, and *P*(14), 1029 cm<sup>-1</sup>, are indicated on each spectrum

$0.100 \pm 0.004$  Torr of reactant using the telescoped beam of a  $\text{CO}_2$  TEA laser at the photolysis source. At both frequencies and with each isotopomer, the extent of reaction up to at least 25% conversion was well described by an equation analogous to a first-order decay,  $[\text{DEC}]_n/[\text{DEC}]_0 = \exp(-kn)$ , where  $n$  is the number of pulses and  $k$  is the fraction of DEC decomposed per pulse within the irradiated volume. The irradiated volume was estimated from cell dimensions and the laser beam diameter observed on thermal paper placed at the entrance window. Values of  $k$  are given in Table 1. At  $0.400$  Torr of reactant some deviations from this apparent first-order behavior were observed. Since reaction produces three molecules of product per decomposed reactant, significant pressure changes occur over the course of the reaction. As products are formed the ambient pressure increases and reaction occurs less efficiently, and this effect becomes signifi-

cant at lower conversions when the initial pressure is increased.

For the same frequency and at identical fluences, the decomposition rate constants for DEC- $d_0$ , DEC- $d_5$  and DEC- $d_{10}$  are very different. These differences are in accord with expectations based on the single photon absorption spectra (see above). Thus, at  $1029 \text{ cm}^{-1}$  the strongest absorber, DEC- $d_0$ , reacts faster than either DEC- $d_5$  or DEC- $d_{10}$ . Similarly, at  $1052 \text{ cm}^{-1}$ , where DEC- $d_{10}$  is the strongest absorber, it is the most reactive. At both frequencies, the reactivities of DEC- $d_5$  is intermediate between those of DEC- $d_{10}$  and DEC- $d_0$ .

The dependence of reaction yields on fluence is also unexceptional. Figure 2 shows yield vs fluence behavior for DEC- $d_0$  at  $P(38)$ ,  $1029 \text{ cm}^{-1}$ , and DEC- $d_5$  at both  $P(38)$ ,  $1029 \text{ cm}^{-1}$ , and  $P(14)$ ,  $1052 \text{ cm}^{-1}$ . The slopes of these plots are DEC- $d_0$   $P(38) = 5.3$ , DEC- $d_5$   $P(14) = 4.4$  and DEC- $d_5$   $P(38) = 5.4$ . These values are

Table 1. Percentage conversion of DEC- $d_n$  in laser beam per pulse

Laser frequency	DEC- $d_0$	DEC- $d_5$	DEC- $d_{10}$
$P(14)^a$	$\ll 0.10$	$4.29 \pm 0.12$	$6.51 \pm 0.95$
$P(38)^b$	$6.12 \pm 1.05$	$1.14 \pm 0.10$	$1.08 \pm 0.06$

<sup>a</sup>  $0.100 \pm 0.004$  Torr DEC- $d_n$ ,  $1.29 \pm 0.02 \text{ J cm}^{-2}$ .

<sup>b</sup>  $0.100 \pm 0.004$  Torr DEC- $d_n$ ,  $1.49 \pm 0.02 \text{ J cm}^{-2}$ .

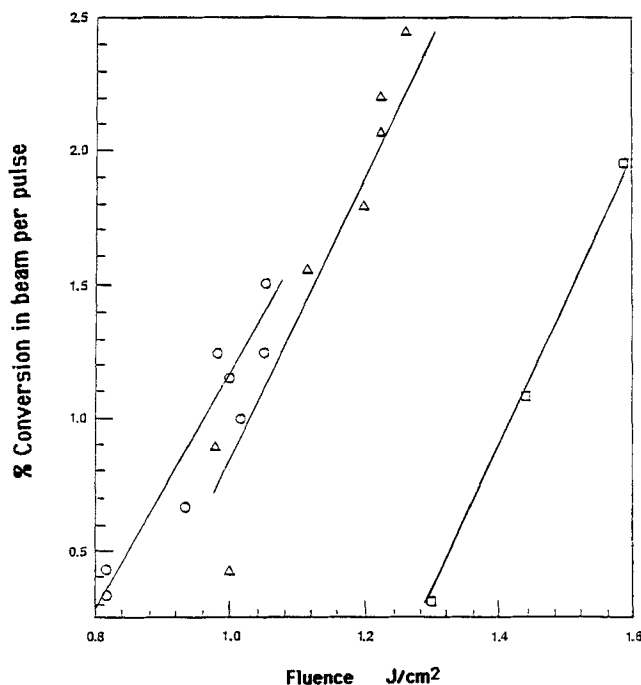


Figure 2. Yield vs fluence for ( $\Delta$ ) DEC- $d_0$   $P(38)$ , ( $\square$ ) DEC- $d_5$   $P(38)$  and ( $\circ$ ) DEC- $d_5$   $P(14)$

in good agreement with work on ethyl acetate under similar conditions. Danen and Jang<sup>13</sup> reported a slope of *ca* 4.2 in the intermediate fluence range (*ca* 1 J cm<sup>-2</sup>) when the reaction probability is of the order of 10<sup>-2</sup> as it is here. Higher fluences are required at *P*(38) than at *P*(14) to achieve comparable conversion of DEC-*d*<sub>5</sub>. Nevertheless, the slope of the fluence vs percentage conversion plot is not significantly different within experimental error at these two frequencies.

Both total yields and branching ratios ( $k_H/k_D$ , Scheme 1) for the photodecomposition of DEC-*d*<sub>5</sub> were determined. A comparison of branching ratios at the two experimental frequencies reveals interesting differences. Data are given in Table 2. When the total yields are identical (entry 2 vs entry 5), the branching ratio is considerably smaller for reaction at *P*(14) ( $\beta = 1.26 \pm 0.17$ ) than for reaction at *P*(38) ( $\beta = 1.63 \pm 0.15$ ). In spite of scatter in the data, these two values are significantly different in the 99.9% confidence level by a standard *t*-test [the total number of degrees of freedom was 19; 8 runs at *P*(38), 13 runs at *P*(14)]. When the two frequencies are compared at the same fluence (entry 4 vs entry 5), the differences are even greater. Clearly, the average reacting molecule absorbs more photons during irradiation at *P*(14) than at *P*(38) under otherwise identical conditions.

RRKM theory has been used to calculate the branching ratio from DEC-*d*<sub>5</sub> as a function of internal energy. The general formulation for using RRKM theory to calculate a branching ratio,  $\beta$ , in this way is given by

$$\beta = \frac{[C_2H_4]}{[C_2D_4]} = \frac{k_H}{k_D} = \frac{\sum_E^\infty N(E)k_H(E)}{\sum_E^\infty N(E)k_D(E)}$$

where  $N(E)$  is the number of reactant molecules that decompose at energy  $E$ ,  $k_H(E)$  and  $k_D(E)$  are RRKM-calculated unimolecular rate constants for a reactant activated to internal energy  $E$  and  $E_0$  is the threshold for reaction. Assuming a delta distribution among reacting molecules,  $\beta = k_H(E)/k_D(E)$ .

The best fit of calculated to observed values of  $\beta$  gives  $\langle E_r \rangle$ , the mean internal energy of reacting molecules. Parameters for the calculation of individual RRKM rate constants,  $k_{H(D)}(E)$ , are given in the Appendix.

The calculations use Arrhenius parameters for the two channels that we determined in an independent series of pyrolysis experiments.<sup>17</sup> The RRKM calculations using the parameters described in the Appendix reproduce the temperature dependence of both the high-pressure rate constant for DEC-*d*<sub>5</sub> disappearance and the branching ratio in the thermal experiments to within the experimental accuracy.

The results of the RRKM calculations are shown in Figure 3. The solid line shows branching ratios ( $\beta$ ) calculated using threshold energies for the two channels,  $E_{0H}$ ,  $E_{0D}$ , determined from thermal activation energies. The broken lines represent values of  $\beta$  for  $E_{0H}$  and  $E_{0D} + \sigma$  and  $E_{0H}$ ,  $E_{0D} - \sigma$ , where  $\sigma$  is the standard deviation of the difference in activation energies from the thermal experiments. Clearly, the calculated branching ratio is sensitive to small changes in the threshold energy difference. The calculation is much less sensitive to other parameters. The best fit of the observed to cal-

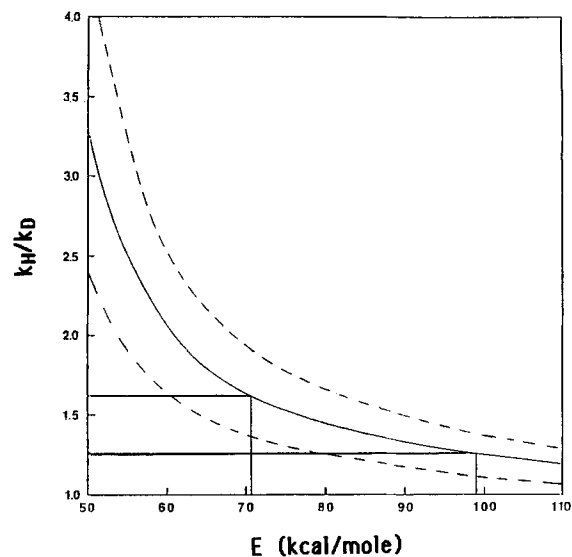


Figure 3. Branching ratio ( $k_H/k_D$ ) vs internal energy for DEC-*d*<sub>5</sub>. Best fits to *P*(14) and *P*(38) data are shown. Broken curves represent upper and lower limits for calculated branching ratio based on error limits of  $E_D$  (see text)

Table 2. Yields and branching ratios in DEC-*d*<sub>5</sub> IR photochemistry

Frequency (cm <sup>-1</sup> )	Fluence (J cm <sup>-2</sup> )	Yield per pulse (%)	Branching ratio, C <sub>2</sub> H <sub>4</sub> /C <sub>2</sub> D <sub>4</sub>
1052 <i>P</i> (14)	0.86 ± 0.02	0.5 ± 0.2	1.51 ± 0.15
1052 <i>P</i> (14)	1.00 ± 0.02	1.0 ± 0.3	1.26 ± 0.17
1052 <i>P</i> (14)	1.32 ± 0.02	2.5 ± 0.3	1.12 ± 0.10
1052 <i>P</i> (14)	1.40 ± 0.02	2.9 ± 0.2	1.09 ± 0.10
1052 <i>P</i> (38)	1.44 ± 0.04	1.0 ± 0.3	1.63 ± 0.15

culated branching ratio gives  $\langle E_T \rangle = 99 \text{ kcal mol}^{-1}$  at  $P(14)$  and  $\langle E_T \rangle = 71 \text{ kcal mol}^{-1}$  at  $P(38)$ . The absolute magnitudes of these energies have fairly large uncertainty owing to the uncertainty in the Arrhenius parameters. However, their differences,  $\langle E_T \rangle_{P(14)} - \langle E_T \rangle_{P(38)}$ , is at least  $20 \text{ kcal mol}^{-1}$ .

There are two important implications of these data. First, yield vs fluence plots for DEC- $d_0$  or DEC- $d_5$  at either frequency are very similar to yield/fluence data for a variety of other 'large' molecules.<sup>13,25,26</sup> These data could surely be successfully fitted by an approximate rate equation model of the type that has been used to rationalize very similar yield data in a number of single-channel multiphoton decomposition experiments.<sup>12c,13,26</sup> Basically these models describe how the energy distribution function of the absorbing population evolves with time. Because the complete rate equation matrix is difficult to solve, models are usually applied to the data in some approximate form. Since the basic elements of the theoretical model are well established, the most important remaining questions concern what approximations can be made that retain the chemically significant effects. For example, an approximate model, which is very appealing in its simplicity, has been suggested by Danen and Jang.<sup>13</sup> This model has been used to rationalize simultaneously bulk absorption and yield/fluence data for several organic esters.<sup>13,27</sup> Multiphoton activation is presumed to produce a Boltzman distribution of internal energies among reactant molecules within the irradiated volume. All reaction occurs after the pulse from the high-energy tail of this distribution. Molecules with sufficient energy such that unimolecular reaction rates (RRKM) are greater than the collisional deactivation rates are assumed to react. Increased fluence raises the average energy of the Boltzman distribution, which increases the population in the tail and thereby the yield.

This model yields the clear prediction that changes in yield which result from variations in laser parameters (fluence, intensity, frequency) must always be accompanied by changes in branching ratio and vice versa. This result is required because the only parameter remaining in the model that is sensitive to irradiation conditions is the average energy of the entire ensemble  $\langle E \rangle$ . Any set of frequency-fluence conditions that produces a given yield must also, according to this one-parameter model, produce a unique branching ratio. In fact, the same conclusion applies to any approximate master equation treatment that assumes a homogeneous ensemble of absorbers, a statistical theory for reaction rate constants and a simple functional form such as  $R_{ij} = I\sigma_0 \exp(-\gamma E_i)$  for the absorption rates, where  $\gamma$  is independent of frequency. To fit the DEC- $d_5$  data, a model must be able to change simultaneously both the average energy and the shape of the ensemble distribution function when frequency and fluence are changed.

Two *ad hoc* ways to build the required flexibility into the model would be first to postulate an inhomogeneous sample incorporating subsets of absorbing ('hot') molecules and non-absorbing ('cold') molecules,<sup>28,29</sup> and allow the relative populations of the subsets to change with frequency. In the case of DEC- $d_5$ , a larger fraction of the sample would be required in the absorbing (hot) population at  $P(38)$  but, because of the smaller value of  $I\sigma_0$ , the average energy of the absorbing population lags behind that for  $P(14)$ . Secondly, permit  $\gamma$  to be frequency dependent.<sup>25</sup> At  $P(14)$ ,  $\gamma$  may be negative and  $R_{ij}$  therefore an increasing function of energy. At  $P(38)$ ,  $\gamma$  could be positive and  $R_{ij}$  therefore a decreasing function of energy. These differences will tend to produce a broader, higher energy distribution for molecules that react at  $P(14)$  and one that is bunched at lower energies for  $P(38)$ . There may be some physical justification for a difference of this type in the energy dependence of the  $P(14)$  and  $P(38)$  absorption cross-sections. Rossi *et al.*<sup>25</sup> showed that for  $C_3F_7I$  the absorption spectrum at high energies has the same features as the small signal absorption spectrum but is red-shifted by *ca*  $20 \text{ cm}^{-1}$ . A progressive red shift in the DEC- $d_5$  spectrum would lead to continuously decreasing cross-sections at  $P(38)$  but sharply increasing cross-sections at  $P(14)$  over  $20 \text{ cm}^{-1}$  of red shift. Independent of the details required to fit the DEC- $d_5$  data successfully with an approximate model, the first implication is that the simplest approximations that have been usefully applied to single-channel reactants are probably not adequate for branching systems, at least over a range of reaction conditions. More remains to be learned about up-pumping rates,  $R_{ij}$ , and the characteristics of the ensemble energy distribution before models can be considered to be predictive, especially for chemically interesting cases involving multiple reactant channels.

The second implication of the branching ratio data is that  $\langle E_T \rangle$  at these two frequencies is very different even when the total yields are the same. The best fitting branching ratios in Figure 3 correspond to the absorption of *ca* 24 and *ca* 34 photons at  $P(14)$  and  $P(38)$ , respectively. The total unimolecular rate constants ( $k_H + k_D$ ) at these energies differ by about two orders of magnitude:  $k\langle E_T \rangle_{P(14)} = 9.0 \times 10^4 \text{ s}^{-1}$  and  $k\langle E_T \rangle_{P(38)} \approx 1.1 \times 10^7 \text{ s}^{-1}$ . It is becoming increasingly apparent that very large differences in the mean unimolecular reaction rate constant can be achieved with fairly modest alterations to the reaction conditions in multiphoton excitation experiments. In addition to these data, recent work on other branching systems has shown differences of over three orders of magnitude in  $k\langle E_T \rangle$  in response to bath gas pressure changes for  $CH_2DCH_2Cl^2$  and approximately two orders of magnitude in response to laser intensity with ethyl vinyl ether.<sup>10</sup> These observations foster the hope that once the details of pressure, intensity and frequency effects in

infrared multiphoton excitation are known, it can become a flexible method for activating chemical reactions capable of delivering known and variable amounts of energy to specific components of reacting mixtures.

## APPENDIX

RRKM rate constants for each reaction channel from DEC-*d*<sub>5</sub> were calculated from the equation<sup>30</sup>

$$k_a(E^*) = L \frac{Q_1^+}{Q_1} \frac{\sum_{E^*=0}^{E^*} P(E_{VR}^*)}{N^* E^*}$$

where

$L^*$  = reaction path degeneracy = 3;

$Q_1^+/Q_1$  = ratio of adiabatic partition functions = 1;

$\sum_{E^*=0}^{E^*} P(E_{VR}^*)$  = sum of vibrational states of the activated complex from the threshold energy  $E_0$  to  $E^*$ ;

$N^*(E^*)$  = density of vibrational states of the reactant at internal energy  $E^*$ .

State sums and densities were calculated using the algorithm described by Stein and Rabinovitch.<sup>31</sup> All internal degrees of freedom were assumed to be harmonic oscillators. Frequencies for DEC-*d*<sub>5</sub> were chosen based on normal mode assignments for dimethyl car-

bonate<sup>32</sup> and characteristic frequencies for carbonate skeletons.<sup>33</sup> Harmonic oscillator approximations to torsional frequencies were calculated from

$$\nu = \frac{n}{2\pi} \left( \frac{V_0}{I_r} \right)^{1/2}$$

using estimates for  $V_0$  and  $I_r$ . These frequencies give a value for  $\Delta S_{(600)}^\ddagger$  in good agreement with group additivity calculations.<sup>34</sup> Frequencies for the activated complexes were obtained by dropping a C-C-O bending mode as the reaction coordinate and adjusting the torsional frequencies to fit the experimental values of  $\Delta S^\ddagger$ . Frequencies are listed in Table 3.

Arrhenius parameters were determined from pyrolysis experiments:<sup>17</sup>  $\log k_H = 12.6 - 43300/\phi$ ;  $\log k_D = 12.7 - 44400/\phi$  ( $\phi = RT$ ). Values of the critical energies,  $E_0$ , were calculated from the Arrhenius activation energies. RRKM calculations were carried out over a range of critical energy differences,  $\Delta E_{0(D-H)}$ , that reflected the error in the thermal data<sup>17</sup>. High-pressure thermal rate constants and branching ratios calculated with RRKM theory using these parameters are in excellent agreement with the pyrolysis data.

## ACKNOWLEDGEMENTS

The authors are grateful for the financial support of the US Department of Energy (DE-AC02-80ER-10592) and the Research Corporation. M.W.T. thanks Henkel and DuPont for summer fellowship support. The authors are grateful to Sidna M. Tulledge for the synthesis of DEC-*d*<sub>5</sub> and DEC-*d*<sub>10</sub>.

## REFERENCES

1. W. E. Farneth, M. W. Thomsen, N. L. Schultz, M. A. Davies, *J. Am. Chem. Soc.* **103**, 4001 (1981).
2. P. J. Papagiannakopoulos, K. Kosnik and S. W. Benson, *Int. J. Chem. Kinet.* **14**, 327 (1982).
3. A. J. Grimley and J. C. Stephenson, *J. Chem. Phys.* **74**, 447 (1980).
4. F. D. Lewis, P. Teng and E. Weitz, *J. Am. Chem. Soc.* **108**, 2818 (1986).
5. Y. Ishikawa, K. Sugita and S. Arai, *J. Phys. Chem.* **90**, 5067 (1986).
6. R. B. Hall and A. Kaldor, *J. Chem. Phys.* **70**, 4027 (1979).
7. V. Starov, N. Selamoglu and C. Steel, *J. Phys. Chem.* **85**, 320 (1981).
8. H. Hofmann, W. Kloepfler, G. Schaefer and J. Gloor, *Chem. Phys.* **56**, 337 (1981).
9. C. Reiser, F. M. Lussier, C. C. Jensen and J. I. Steinfeld, *J. Am. Chem. Soc.* **101**, 350 (1979).
10. D. M. Brenner, *J. Phys. Chem.* **41**, 86 (1982).
11. (a) M. Quack, *J. Chem. Phys.* **69**, 1282 (1978). (b) M. Quack, in *Laser-Induced Processes in Molecules*, edited by K. Kompa and S. D. Smith, pp. 142-144. Springer, Berlin (1979).

Table 3. Frequencies and degeneracies for RRKM calculations

DEC- <i>d</i> <sub>5</sub> (cm <sup>-1</sup> )	$k_H$ (transition state)	$k_D$ (transition state)
3000 (5)	3000 (5)	3000 (5)
2150 (5)	2150 (5)	2150 (5)
1760	1760	1760
1430 (2)	1430 (2)	1430 (2)
1295	1295	1295
1150 (3)	1150 (3)	1150 (3)
1060 (3)	1060 (3)	1060 (3)
1030 (2)	1030 (2)	1030 (2)
1025	1025	1025
1000 (2)	1000 (2)	1000 (2)
990	990	990
950 (3)	950 (3)	950 (3)
857	857	857
801	801	801
634	634	634
579	579	579
518	518	518
400 (2)	400	400
222	320	222
190	190	260
90	140	90 (2)
70	70	60 (2)
60	75	
50	50	

12. (a) J. R. Barker and A. C. Baldwin, *J. Chem. Phys.* **74**, 3813 (1981); (b) D. M. Golden, M. J. Rossi, A. C. Baldwin and J. R. Barker, *Acc. Chem. Res.* **14**, 56 (1981); (c) A. C. Baldwin and J. R. Barker, *J. Chem. Phys.* **74**, 3823 (1981).
13. W. C. Danen and J. C. Jang, in *Laser-Induced Chemical Processes*, edited by J. I. Steinfeld, pp. 45–159 Plenum Press, New York (1981).
14. (a) J. L. Buechele, E. Wertz and F. D. Lewis *J. Am. Chem. Soc.* **103**, 3588 (1981); (b) A. Ben-Shaul and Y. Haas, *J. Chem. Phys.* **73**, 5107 (1980).
15. W. H. Richardson, and H. E. O'Neal, in *Comprehensive Chemical Kinetics*, edited by C. J. Bamford and C. F. H. Tipper, Vol. 5, p. 381. Elsevier, Amsterdam (1972).
16. (a) A. S. Gordon and W. P. Norris, *J. Phys. Chem.* **69**, 3013 (1965); (b) D. B. Bigley and C. M. Wren, *J. Chem. Soc., Perkin Trans. 2*, 926 (1972); (c) J. T. D. Cross, R. Hunter and V. R. Stimson, *Aust. J. Chem.* **29**, 1477 (1976).
17. W. E. Farneth and T. L. Beck *Int. J. Chem. Kinet.* **15**, 461 (1983).
18. (a) W. C. Danen, W. D. Munslow, and D. W. Setser, *J. Am. Chem. Soc.* **99**, 6961 (1977); (b) W. C. Danen, V. C. Rio and D. W. Setser, *J. Am. Chem. Soc.* **104**, 5431 (1982).
19. J. E. Eberhardt, R. B. Knott, A. W. Pryor and R. G. Gilbert, *Chem. Phys.* **69**, 45 (1982).
20. J. March, in *Advanced Organic Chemistry*, 2nd ed., p. 926. McGraw-Hill, New York (1977).
21. J. P. Perchard and M. L. Josien, *J. Chem. Phys.* **65**, 1834, 1856. (1963).
22. M. Haurie and A. Novak, *J. Chem. Phys.* **62**, 146 (1965).
23. B. Nolen and R. N. Jones, *Can. J. Chem.* **34**, 1392 (1956).
24. N. B. Colthup, L. H. Daly and S. E. Wiberley, in *Introduction to Infrared and Raman Spectroscopy*, P. 379. Academic Press, New York (1977).
25. M. J. Rossi, J. R. Barker and D. M. Golden, *J. Chem. Phys.* **76**, 406 (1982).
26. P. A. Schulz, A. S. Sudbo, P. J. Krajnovich, H. S. Kwok Y. R. Shen and Y. T. Lee, *Annu. Rev. Phys. Chem.* **30**, 379 (1979), and reference cited therein.
27. H. H. Nguyen and W. C. Danen, *J. Am. Chem. Soc.* **103**, 6253 (1981).
28. Y. S. Doljikov, V. S. Letokhov, A. L. Makarov and E. A. Ryabov, *Chem. Phys. Lett.* **124**, 304 (1986).
29. R. J. McCloskey, S. V. Babu, *J. Phys. Chem.* **86**, 3210 (1982).
30. P. J. Robinson and K. A. Holbrook, in *Unimolecular Reactions*, P. 64ff. Wiley-Interscience, London (1972).
31. S. E. Stein and B. S. Rabinovitch, *J. Chem. Phys.* **58**, 2438 (1973).
32. B. Collingwood, H. Lee and J. K. Wilmshurst, *Aust. J. Chem.* **19**, 1637 (1966).
33. A. R. Katritzky, J. M. Lagowski and J. A. T. Beard, *Spectrochim Acta* **16**, 954 (1960).
34. S. W. Benson, in *Thermochemical Kinetics*. Wiley, New York (1976).